Influence of NiO on the crystallization kinetics of near stoichiometric cordierite glasses nucleated with TiO_2

2007 J. Phys.: Condens. Matter 19 386231

(http://iopscience.iop.org/0953-8984/19/38/386231)

IOP PUBLISHING JOURNAL OF PHYSICS: CONDENSED MATTER

J. Phys.: Condens. Matter **19** (2007) 386231 (14pp) doi:10.1088/0953-8984/19/38/386231

Influence of NiO on the crystallization kinetics of near stoichiometric cordierite glasses nucleated with TiO_2

Ashutosh Goel[1], Essam R Shaaban[2], Manuel J Ribeiro[3], Francisco C L Melo[4] and José M F Ferreira[1,5]

[1] Department of Ceramics and Glass Engineering, University of Aveiro, CICECO, 3810-193 Aveiro, Portugal
[2] Physics Department, Faculty of Science, Al-Azhar University, Assuit 71542, Egypt
[3] UIDM, ESTG, Polytechnic Institute of Viana do Castelo, 4900 Viana do Castelo, Portugal
[4] Centro Técnico Aeroespacial, Instituto de Aeronáutica do Espaço, Divisão de Materiais, S José dos Campos–SP, Brazil

E-mail: jmf@ua.pt

Received 21 May 2007, in final form 6 July 2007
Published 4 September 2007
Online at stacks.iop.org/JPhysCM/19/386231

Abstract

This work presents the effect of NiO on the thermal behavior and the crystallization kinetics of glasses lying near the stoichiometric cordierite composition nucleated with TiO_2. Three glasses with NiO content varying between 1 and 5 mol% have been synthesized in Pt crucibles. Activation energies for structural relaxation and viscous flow have been calculated using the data obtained from differential thermal analysis (DTA). Kinetic fragility of the glasses along with other thermal parameters has been calculated. Non-isothermal crystallization kinetic studies have been employed to study the mechanism of crystallization in all three glasses. The crystallization sequence in the glasses has been followed by x-ray diffraction analysis of the heat treated glass samples in the temperature range of 800–1200 °C. μ-cordierite has been observed to be the first crystalline phase in all the glass samples after heat treatment at 850 °C, while NiO plays an important role in determining the crystallization sequence at higher temperatures, leading to the formation of α-cordierite.

1. Introduction

Between the end members of the SiO_2–$MgAl_2O_4$ join, there is a point corresponding to the ternary compound $Mg_2Al_4Si_5O_{18}$, a cordierite showing complex polymorphism. Cordierite glass-ceramics belong to an important class of advanced technological materials having a wide range of applications [1–3]. Cordierite ($2MgO–2Al_2O_3–5SiO_2$) and cordierite-based glass-ceramics have been extensively studied in various applications including ceramic matrix composites (CMCs) [4, 5] and substrates for high speed computers [6, 7] mainly due to their beneficial properties, i.e. low thermal expansion coefficient, low dielectric constant and high

[5] Author to whom any correspondence should be addressed.

chemical durability [8–11]. These glass–ceramics are interesting candidates for a number of elevated temperature applications where good high temperature creep resistance coupled with a high resistance to thermal shock is required [12, 13].

Glass–ceramics with transition metal ions incorporated within their crystalline phases are important because of their potential technological applications. Among the transition metal ions, Ni^{2+} is an interesting candidate and the phase formation in the $MgO–Al_2O_3–SiO_2–NiO$ system has important technological implications that find applications in electric engineering, and as special refractories and catalyst carriers.

Previous studies concerning the crystallization pathway of NiO doped magnesium aluminosilicate glasses and Mg-cordierite glasses have been reported. Golubkov *et al* [14, 15] investigated the effect of the addition of NiO on the phase separation and crystallization of the magnesium aluminosilicate glasses with equimolar contents of MgO and Al_2O_3 nucleated by TiO_2 and doped by 0.5–5 mol% NiO. They observed the reduction in crystallization ability of the magnesium aluminotitanate phase with an increase in the content of NiO leading to its complete suppression in the presence of 5 mol% NiO. Alekseeva *et al* [16] studied the phase transformations in NiO doped magnesium aluminosilicate glasses nucleated by ZrO_2 and reported on the change in the absorption spectra of the material due to the entrance of the Ni^{2+} ions in the aluminosilicate crystalline phases. Boberski and Giess [17] studied the isothermal crystallization behavior of the stoichiometric powdered cordierite glasses containing NiO and found the existence of a complete crystalline solid solution between magnesium cordierite ($Mg_2Al_4Si_5O_{18}$) and nickel cordierite ($Ni_2Al_4Si_5O_{18}$). They also concluded that the formation of nickel containing cordierite was independent of the nickel content in the glass. The effect of the NiO on the crystallization of glasses in the $MgO–Al_2O_3–SiO_2$ system was also reported by Doenitz and Vogel [18]. The authors claimed that the presence of NiO could change the crystallization mechanism.

Despite these very interesting studies aimed specifically at examining the influence of NiO on the relationship between phase separation, nucleation and crystallization in the $MgO–Al_2O_3–SiO_2$ glasses, in general, and cordierite glasses, in particular, a literature survey reveals that no studies have been made so far dealing with the effect of NiO on the thermal stability and non-isothermal crystallization kinetics of the cordierite glasses nucleated with TiO_2. Therefore, more comprehensive data is required before a clearer understanding of the crystallization processes can emerge.

In view of the above mentioned perspective, the aim of the present work is to investigate the influence of NiO on the thermal stability and crystallization kinetics of the near stoichiometric cordierite glasses nucleated with TiO_2 by means of differential thermal analysis (DTA) and x-ray diffraction (XRD). Table 1 presents the details of the three investigated compositions, designated as MAST-N1, MAST-N3 and MAST-N5. The compositions were designed in such a manner as to increase the content of NiO while keeping constant the molar ratios of all the other constituent oxides. Note that the label MAST derives from our previous study [19] dealing with the non-isothermal crystallization kinetics of the cordierite glass nucleated with 5 mol% TiO_2. Further, N1, N3 and N5 designate the concentration of NiO (i.e. 1, 3 and 5 mol%) in the glasses investigated in the present study.

2. Experimental procedure

2.1. Sample preparation

Powders of technical grade SiO_2 (purity > 99.5%), and of reactive grade Al_2O_3, $MgCO_3$, TiO_2 and NiO, were used. Well mixed batches (∼100 g), according to table 1, obtained by ball

Table 1. Batch compositions of parent glasses.

Glass		MgO	Al_2O_3	SiO_2	TiO_2	NiO
MAST-N1	wt%	12.93	32.70	48.37	4.87	1.14
	mol%	20.99	21.15	52.79	4.07	1.00
	mol ratio	1	1	2.51	0.19	0.05
MAST-N3	wt%	12.63	31.95	47.26	4.75	3.40
	mol%	20.57	20.72	51.72	3.99	3.00
	mol ratio	1	1	2.51	0.19	0.15
MAST-N5	wt%	12.33	31.20	46.16	4.64	5.66
	mol%	20.15	20.30	50.65	3.90	5.00
	mol ratio	1	1	2.51	0.19	0.25

milling, were preheated at 900 °C for 1 h for decarbonization and then melted in Pt crucibles at 1580 °C for 1 h, in air.

Glasses in bulk form were produced by pouring the melts on preheated bronze moulds following by annealing at 550 °C for 1 h. The samples of the glass powders were produced from glass frits, which were obtained by quenching glass melts in cold water. The frits were dried and then milled in a high-speed agate mill, resulting in fine glass powders with mean particle sizes of 5.02–5.45 μm (determined by the light scattering technique; Coulter LS 230, UK; Fraunhofer optical model). The true density of the glass powders, obtained after milling the glass frits, was measured by a Quantachrome multipycnometer based on the Archimedes principle of fluid displacement (employing helium gas as the fluid).

2.2. Sample characterization

Dilatometry measurements on the bulk glasses were made with prismatic samples with cross section of 4×5 mm^2 (Bahr Thermo Analyse DIL 801 L, Germany; heating rate 5 K min^{-1}). The coefficient of thermal expansion (CTE) values for all the bulk glasses was obtained from the linear portion of the dilatation curve in the temperature range of 200–500 °C.

Crystallization kinetics of the glasses was studied using differential thermal analysis (Netzsch 402 EP, Germany). The glass powder weighing 50 mg was contained in an alumina crucible and the reference material was α-alumina powder. The samples were heated in air from ambient temperature to 1200 °C at heating rates (β) of 5, 10, 20, 25 and 30 K min^{-1}. The value of the glass transition temperature T_g, crystallization onset temperature, T_c, and peak temperature of crystallization, T_p, were determined by using the microprocessor of the thermal analyzer.

To follow the crystallization sequence of the investigated glasses, the bulk annealed glasses were cut into small pieces ($\sim$5 mm thick and $\sim$5 mm long) and heat treated in an electric furnace in air at different temperatures varying between 800–1200 °C, followed by a soaking time of 1 h. The heating rate was 5 K min^{-1}. The crystalline phases were identified by x-ray diffraction analysis (XRD, Rigaku Geigerflex D/Mac, C Series, Cu Kα radiation, Japan). Copper Kα radiation ($\lambda = 1.5406$ nm) produced at 30 kV and 25 mA scanned the range of diffraction angles (2θ) between 10° and 80° with a 2θ-step of 0.02°s^{-1}. The phases were identified by comparing the experimental x-ray patterns to standards complied by the International Centre for Diffraction Data (ICDD).

Microstructure observations were made at fractured bulk glasses and glass–ceramics, etched by immersion in 4 vol% HF solution for different time durations (the glasses were etched for 10 s while the glass–ceramics were etched for 90 s), by field emission scanning electron

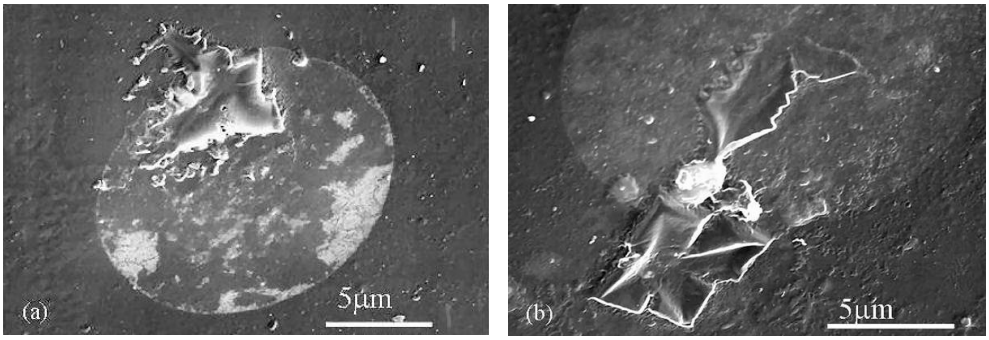

Figure 1. SEM images of the bulk annealed glass MAST-N5 from two different regions.

Table 2. Thermal parameters for the glasses obtained from dilatometry and DTA (figures 2, 3 and 4).

Glass	CTE[a]	$E_{\text{relax.}}$ (kJ mol^{-1})	E_η (kJ mol^{-1})	F	ΔT (K)	S (K)
MAST-N1	4.18	532	515	25.75	90	1.12
MAST-N3	4.45	556	539	27.02	85	1.22
MAST-N5	3.21	599	581	29.34	83	1.36

[a] CTE ($\times 10^{-6}$ K^{-1}) temperature range: (200–500 °C).

microscopy (FE-SEM, Hitachi S-4100, Japan; 25 kV acceleration voltage, beam current 10 μA) under secondary electron mode. Energy dispersive analysis (EDS) was employed to identify the phases in amorphous phase separation in glasses.

3. Results

3.1. Characterization of glasses

For all the investigated compositions, melting at 1580 °C for 1 h was adequate to obtain bubble-free, transparent glasses with a dark honey color (brown). The color of the glass became darker with the increase of NiO content. Absence of crystalline inclusions was confirmed by x-ray diffraction. The values of the real density for the glass powders as calculated using the Multipycnometer are 2.72 ± 0.02, 2.74 ± 0.01 and 2.81 ± 0.01 g cm^{-3} for MAST-N1, MAST-N3 and MAST-N5, respectively. It is evident from these values that the glass density increases with NiO content. Figure 1 shows the SEM image of the bulk annealed glass MAST-N5. A uniform oval shaped region can be seen on the glass surface with a protuberance connecting this oval structure to the glass surface. These types of regions were observed on the glass surface at different points but were not homogeneously distributed.

Along the series of the three investigated NiO-containing compositions of table 1, the property values, summarized in table 2, reveal the following general features.

(a) The CTE value is almost the same for the glasses MAST-N1 and MAST-N3; however, it decreases considerably for glass MAST-N5.
(b) The lowest glass transition temperature (T_g) was registered for the glass MAST-N5 and the highest for MAST-N1 (figure 2). The activation energy for the structural relaxation of the glass occurring around the glass transition was calculated by using the equation [20, 21]

$$\ln \beta = \frac{-E_{\text{relax}}}{RT_g}$$

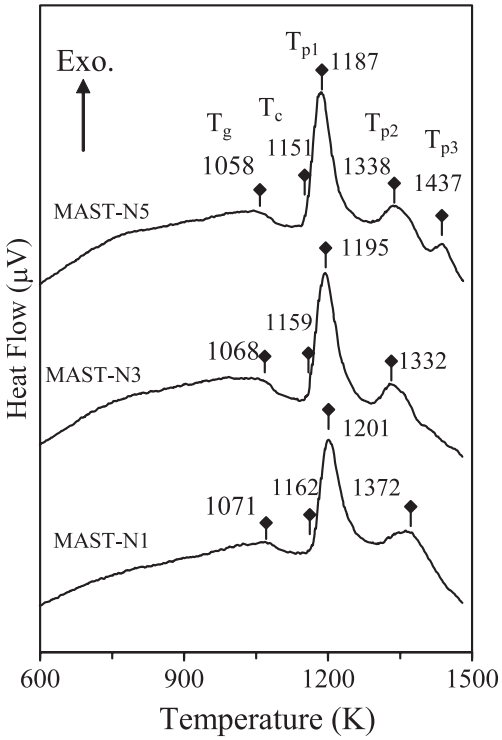

Figure 2. Differential thermal analysis (DTA) data of powders of the investigated glasses heated with a rate of 25 K min^{-1}.

while the activation energy for viscous flow, E_η, was calculated from the equation

$$\ln\left(T_g^2/\beta\right) = E_\eta/RT_g + \text{const.}$$

The activation energy for viscous flow (figure 3) and activation energy for structural relaxation (figure 4) both increase with NiO content in the glasses.

(c) The values of glass fragility index (F) (for the equation, refer to the theoretical background of [19]) tend to increase as the NiO content increases.

(d) The value of thermal stability parameter $\Delta T = (T_c - T_g)$ turns out to be inversely proportional to the NiO content, while that for S [19] is directly proportional to the amount of NiO in the glasses.

3.2. Crystallization of glasses

The DTA plots of fine powders with a heating rate of 25 K min^{-1}, shown in figure 2, feature two well-defined crystallization exotherms for the glasses MAST-N1 and MAST-N3 while glass MAST-N5 exhibited three crystallization exotherms, signifying the appearance of at least two and three different crystalline phases, respectively. This trend was observed for the DTA scans at all the heating rates. The crystallization maximum temperature (T_p) is seen to increase with the increase in heating rate. The peak temperature of crystallization for the formation of the first crystalline phase (T_{p1}) for all the glasses lies in a close range with the highest being 1047 K for MAST-N1 and the lowest being 1035 K for MAST-N5. However, significant differences

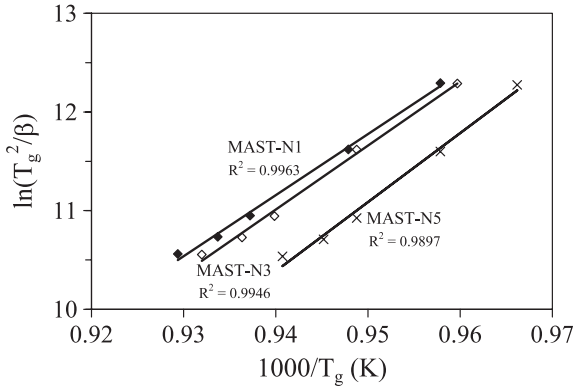

Figure 3. Plot for determination of the activation energy for viscous flow of the investigated glasses (E_η). The values of correlation coefficients (R^2) are also presented.

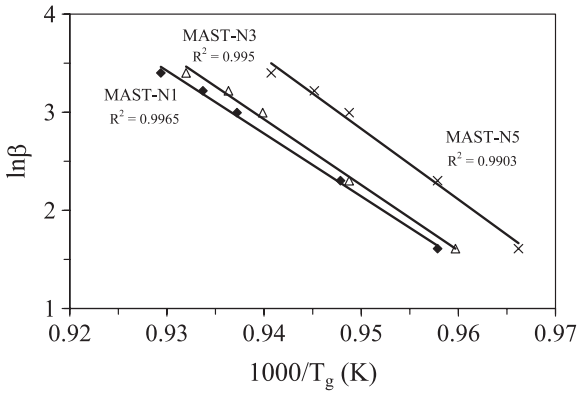

Figure 4. Plot for determination of the activation energy for structural relaxation of the investigated glasses ($E_{\text{relax.}}$). The values of correlation coefficients (R^2) are also presented.

Table 3. Activation energy of crystallization for the glasses (units: kJ mol^{-1}) (figure 5).

Glass	First crystallization peak (E_{c1})	Second crystallization peak (E_{c2})	Third crystallization peak (E_{c3})
MAST-N1	291	510	—
MAST-N3	310	309	—
MAST-N5	315	307	525

in the temperatures can be seen for the emergence of the second (T_{p2}) and the third (T_{p3}) exothermic peaks in all three glasses. The activation energy for crystallization of the glasses was calculated similarly as in our previous study [19], so as to maintain consistency while comparing the results. The values of activation energy of crystallization (figure 5, table 3) are in good agreement with the DTA results. Based on these DTA results, devitrification behavior was studied by non-isothermal heating of bulk glass samples in the temperature range of 800 °C (1073 K)–1200 °C (1473 K) for 1 h. All the glasses were XRD amorphous after heat treatment at 800 °C and no color change was observed in any of the three glasses. Figure 6

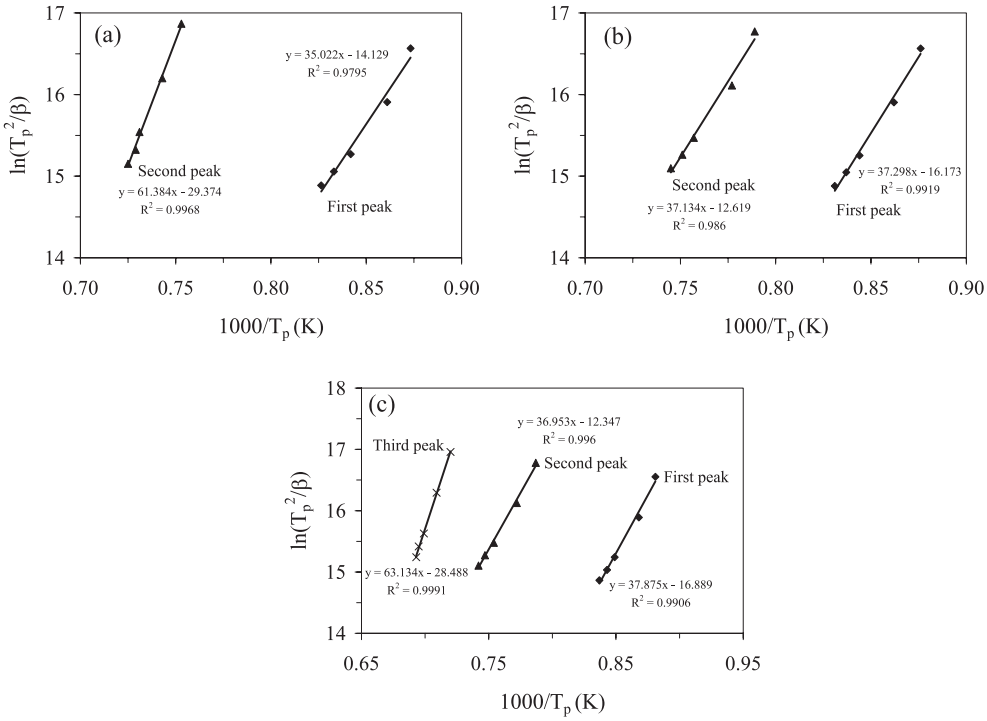

Figure 5. Plots for determination of the activation energy for crystallization of the investigated glasses (E_c): (a) MAST-N1 glass; (b) MAST-N3 glass; (c) MAST-N5 glass. The values of correlation coefficients (R^2) are also presented.

shows the x-ray diffractogram of all three bulk glasses heat treated for 1 h at 850 °C, and at 950 °C and 1000 °C for MAST-N1 and MAST-N3, respectively. Magnesium aluminum silicate (μ-C; PDF No 14-0249), a hexagonal, metastable, solid solution of the quartz type, with a composition similar to that of cordierite, generally known as μ-cordierite, crystallizes out to be the single and primary phase in all three glasses. The color of all the glasses started to change after heat treatment at 850 °C from brown to green depending on the content of NiO. Glass MAST-N5 showed a mixture of green and brown color after heat treatment at 850 °C. At 900 °C, glass MAST-N3 was converted to green color with still a tinge of brown color in it while glass MAST-N5 was totally converted to teal color. The intensity of the strongest peak ($2\theta = 25.833°$) increased with the increase in the amount of NiO (figure 7), thus giving evidence that the DTA results are in good agreement with the XRD results. Upon further heat treatment, α-cordierite or cordierite (C; PDF No 86-1550) appears along with μ-C in glass MAST-N1 at 950 °C (figure 6) without the formation of any other minor crystalline phases. At 1050 °C, glass MAST-N1 was converted to an ivory white color with cordierite as the only crystalline phase. The crystallization mechanism in glasses MAST-N3 and MAST-N5 became more complex due to the appearance of different minor and trace phases along with the shift in the formation of cordierite towards higher temperatures. Orthorhombic magnesium aluminum silicate (MAS*; PDF No 35-310) precipitated out along with μ-C after heat treatment of glass MAST-N3 at 950 °C for 1 h, which was converted to α-cordierite at 1000 °C along with the formation of a spinel (Sp; $MgAl_2O_4$; PDF No 99-0098) (figure 6). μ-C still crystallized out to be the primary phase. Upon further heat treatment at 1050 °C, dissolution of μ-C took place

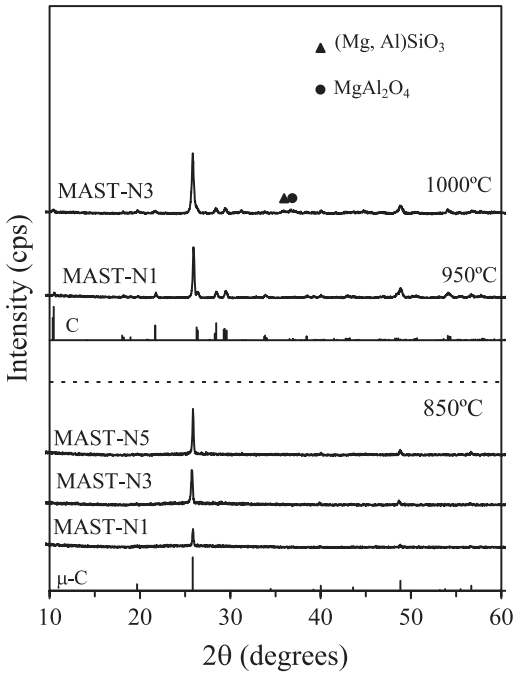

Figure 6. X-ray diffractograms of bulk glasses, after heat treatment at different temperatures for 1 h (for labels, refer to text). The patterns have not been normalized; full scale 7000 cps.

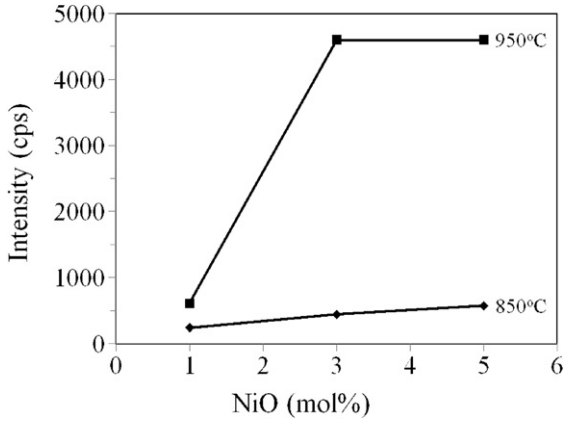

Figure 7. Plot for the variation of intensity of crystalline phase, μ-cordierite, with the increase in NiO content at 850 and 950 °C.

to form cordierite and quartz (Q; PDF No 47-1144) as the primary crystalline phases along with nickel silicate (NS; PDF No 83-1648) as a trace phase. At 1100 °C, cordierite crystallized out to be the only crystalline phase in MAST-N3 while the color of the glass–ceramic changed to turquoise. A more entangled crystallization mechanism is observed for MAST-N5 as some unidentified minor phases are crystallized along with μ-C (primary phase) at 950 °C. Quartz precipitates out to be the primary phase at 1050 °C along with NS. At 1100 °C, sapphirine (S; PDF No 76-0536), crystallized out to be the only phase while all the other phases disappeared.

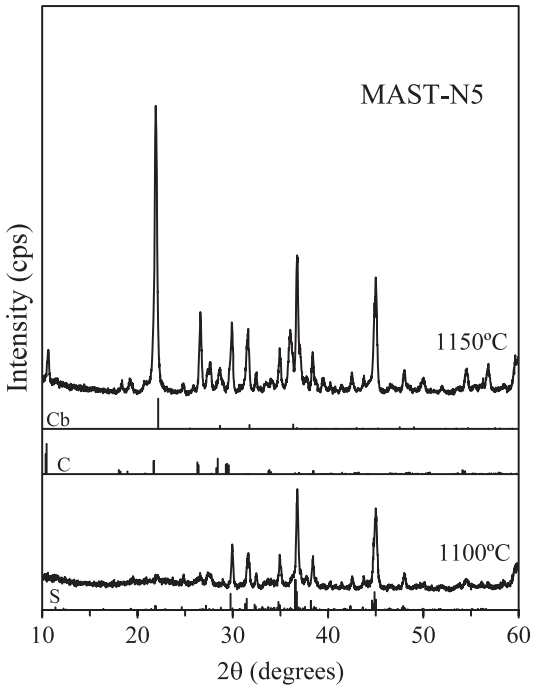

Figure 8. X-ray diffractograms of bulk glass, MAST-N5, after heat treatment at 1100 °C and 1150 °C for 1 h respectively (for labels, refer to text). The patterns have not been normalized; full scale 7000 cps.

Table 4. Crystal phase development in the glasses at different temperatures as determined by XRD. (X: unidentified minor phase.)

Glass	800 °C	850 °C	900 °C	950 °C	1000 °C	1050 °C	1100 °C	1150 °C	1200 °C
MAST-N1	Amorphous	μ-C	μ-C	μ-C; C	μ-C; C	C	C	—	—
MAST-N3	Amorphous	μ-C	μ-C	μ-C; MAS*	μ-C; C; Sp; MAS*	C; Q; NS	C	—	—
MAST-N5	Amorphous	μ-C	μ-C	μ-C; X	μ-C; NS	Q; NS	S	C; S; Cb	C; S; Cb

Heat treatment at 1150 °C led to the formation of cristobalite (Cb; PDF No 82-1405) along with the sapphirine as the primary crystalline phases while cordierite precipitated out as a minor crystalline phase (figure 8). The color of the glass–ceramic changed to light turquoise. Further heat treatment at 1200 °C showed no change in the composition or the intensity of the crystalline phases. Table 4 summarizes the results of the crystal phase development in all three investigated glasses after heat treatment at various temperatures between 800 °C and 1200 °C for time durations of 1 h respectively.

Figure 9 shows the microstructure of the heat treated glasses at different temperatures. At 900 °C, dendritic structure corresponding to μ-cordierite, extending uniformly all over the surface, can be seen in the microstructure of glass MAST-N3. α-cordierite appeared in the form of needle shaped crystals with high aspect ratio in glass MAST-N1 heat treated at 1100 °C, while it appeared in the shape of spherulites in the glass MAST-N3 at 1150 °C. In the sample MAST-N5 heat treated at 1200 °C some larger crystals could be observed among highly dispersed small crystals, supporting the XRD results for the presence of more than one crystalline phase.

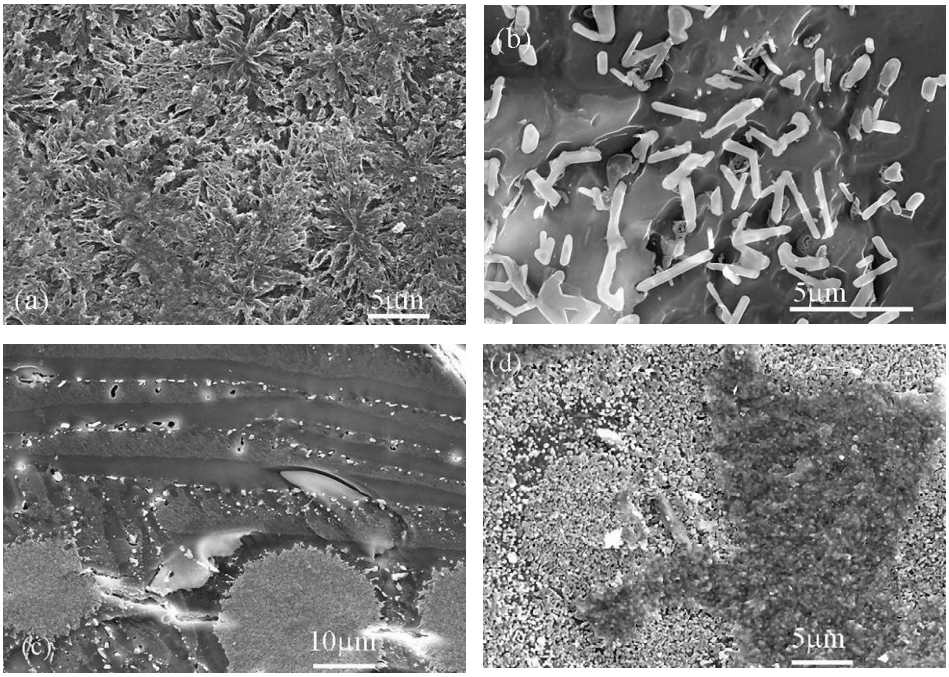

Figure 9. SEM image of glass (a) MAST-N3 heat treated at 900 °C, (b) MAST-N1 heat treated at 1100 °C, (c) MAST-N3 heat treated at 1150 °C, and (d) MAST-N5 heat treated at 1200 °C.

4. Discussion

Nickel is probably one of the elements that imparts to oxide glasses the widest range of coloration: green, yellow, brown, purple, and blue. These modifications of the glass color have been interpreted in the past as arising from two kinds of sites, octahedral and tetrahedral, the proportion of which varies as a function of glass composition [22]. The origin of this brown coloration in the glasses due to NiO has been explained by Calas *et al* [23], according to whom this color arises from the presence of nickel in five coordination, in trigonal bipyramids.

The experimental results showed that incorporation of NiO causes a density increase of the glasses. This is not surprising as NiO has higher density (∼6.72 g cm^{-3}) than most silicate glasses. In our previous study [19], the CTE value for the glass MAST was found to be 4.27×10^{-6} K^{-1} (200–500 °C) which is almost similar to the values obtained for glasses MAST-N1 and MAST-N3 in the present study. However, the CTE value for glass MAST-N5 is considerably lower than the values for all the other investigated glasses. The transition temperature (T_g) for the glasses has also been observed to decrease with increasing NiO contents. This observation of decrease in CTE and T_g with increasing NiO content is consistent with a recent study of Chou *et al* [24] and may be attributed to the formation of larger size inhomogeneous regions in the glasses with increasing NiO contents. Figure 1 is an evident example of formation of such inhomogeneous regions. Also, according to Golubkov *et al* [14], in glasses doped with NiO, at early stages of heat treatment, sizes of inhomogeneous regions and $|\Delta\rho|^2$ (the square of the mean difference of the electronic densities inside the inhomogeneous regions and the glass matrix), rapidly increase; $|\Delta\rho|^2$ is proportional to NiO content. This implies that the phase containing NiO precipitates upon phase decomposition; the structure formed determines the structure of the phase separated materials and of resultant

glass–ceramics. Chou *et al* [24] observed the presence of a heterogeneous mixture of black and green streaks in the core of the bulk annealed Sr-silicate glasses with high content of NiO (∼15 mol%). However, due to the amorphous nature of the glasses (with a high amount of NiO and appreciable amounts of precipitates) as observed from the XRD analysis, they concluded that the precipitates were either amorphous in nature or consisted of very fine particles. The values of F and ΔT for all three investigated glasses support our results. The values of F for the all three glasses show that they have been obtained from KS liquids but the increase of F value with NiO content points towards an enhanced inhomogeneity in the glasses.

The increase in the activation energy of structural relaxation and viscous flow with increase in NiO content may be explained by taking into account the bond strength and ionic radii of the constituent oxides incorporated into the glasses. The bond strength (D^0_{298} kJ^{-1} mol^{-1}) of the MgO, Al_2O_3, SiO_2, TiO_2, and NiO are 363.2 ± 12.6, 511 ± 3, 799.6 ± 13.4, 672.4 ± 9.2, and 382 ± 16.7, respectively, while the Pauling ionic radii (pm) of these oxides are 65, 67.5, 41, 68, and 69, respectively [25]. Since the bond strength of all the oxides (except MgO) is higher and the ionic radii is lower than that for NiO, replacement of any of the constituent oxides by NiO will convert the covalent silicate network into an ionic one, thus increasing both the activation energy for viscous flow (figure 3) and structural relaxation (figure 4). The values of the activation energy for structural relaxation (E_{relax}) occurring around the T_g of the respective glasses are in good agreement with the activation energy for the viscous flow (E_η) of the respective glasses. The crystallization activation energy obtained for the first crystalline phase (E_{c1}) for all three glasses is less than E_{relax} and E_η of the respective glasses. This indicates that the crystallization in all three glasses is more concerned with diffusion processes.

The DTA and XRD results are in good agreement with each other as the first peak of the DTA thermograph for all three glasses corresponds to the formation of μ-C (μ-cordierite). The crystalline phase (μ-C) appears at the same temperature (850 °C) in all three glasses but its intensity constantly increases with the increase in the content of NiO due to the continued liquid-phase separation and crystallization in the precipitated regions (figure 7). Figure 9(a) shows the homogeneous dendritic microstructure for μ-cordierite, thus pointing towards the presence of a single crystalline phase. The activation energy of crystallization (E_{c1}) for μ-C lies in a close range for all three glasses, thus supporting the DTA results. It should be noted that the values of T_{p1} and E_{c1} for all the NiO containing glasses are considerably lower than that for MAST glass ($T_{p1} = 1152$ K, $E_{c1} = 340$ kJ mol^{-1}) and the stoichiometric cordierite glasses doped with B_2O_3 and P_2O_5 [26]. The decrease in the activation energy (E_{c1}) for the three glasses in comparison to the glass MAST could again be explained on the basis of increased phase separation in the NiO-containing glasses. This proves that NiO plays a significant role in altering the crystallization mechanism of the glass. However, from the close agreement in the T_{p1} and E_{c1} values of all three NiO containing glasses, it can be said that the initiation of crystallization in the glasses is independent of the content of NiO.

The ratio between the ordinates of the DTA curve and the total area of the peak gives the corresponding crystallization rates, which makes it possible to build the curves of the exothermal peaks represented in figure 10. It may be observed that the $(dx/dt)_p$ value increases as well as the heating rate, a property which has been widely discussed in the literature [27]. From the experimental values of the $(dx/dt)_p$ one can calculate the kinetic exponent n by using the following equation:

$$(d\chi/dt)_p = n(0.37\beta E_c)/(RT_p^2).$$

The n values for the present glasses are calculated and listed in table 5. The corresponding mean value may be taken as the most probable value of the quoted exponent. Besides, from the mean value of the kinetic exponent, n, it is possible to postulate a crystallization reaction mechanism

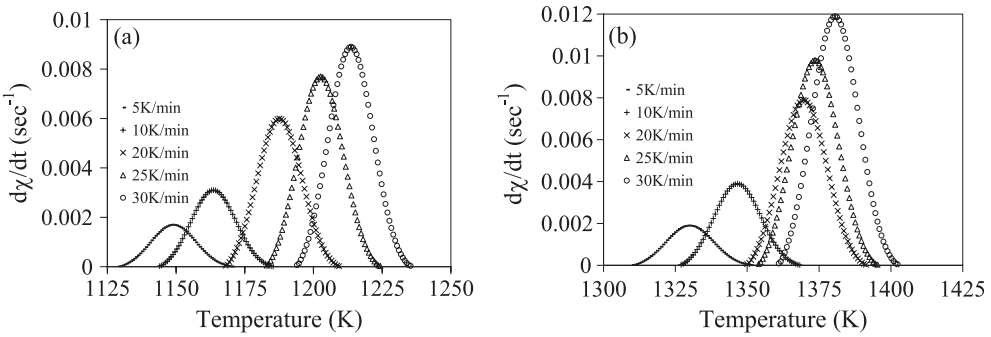

Figure 10. Crystallization rate versus temperature of the (a) first exothermic peak and (b) second exothermic peak at different heating rates for glass MAST-N1. The crystallization curves for glasses MAST-N3 and MAST-N5 showed the same behavior.

Table 5. Avrami parameter, $\langle n \rangle$ for the crystallization curves of the glasses. (Note: subscripts 1, 2 and 3 refer to the first, second and third crystallization exothermic peaks respectively.)

Glass	$\langle n_1 \rangle$	$\langle n_2 \rangle$	$\langle n_3 \rangle$
MAST-N1	2.00 ± 0.06	1.93 ± 0.07	—
MAST-N3	2.97 ± 0.19	2.95 ± 0.09	—
MAST-N5	2.03 ± 0.12	2.09 ± 0.09	1.11 ± 0.04

for the magnesium aluminum silicate glasses. A value of n close to three supports bulk or three-dimensional crystal growth and a value close to unity indicates surface growth. Intermediate values of n between unity and three might result when surface and internal crystallization occur simultaneously. The value of the Avrami parameter for the first crystalline phase $\langle n_1 \rangle$ (table 5) for all the glasses suggests that the crystallization did not occur on a fixed number of nuclei and the crystalline phase, μ-C, grew by simultaneous surface and internal crystallization in glasses MAST-N1 and MAST-N5, while three-dimensional bulk nucleation occurred in MAST-N3. It is also important to note that complications appear with systems where n is a non-integer value and the deviation from the integer value of the Avrami exponent might originate from impurities influencing crystal growth and the simultaneous appearance of different growth mechanisms as well as from the density of the growing phases [28]. μ-C phase continued to be the single existing phase in all three NiO containing glasses up to 900 °C. However, the crystallization mechanism of all three glasses changed with the further increase in temperature depending on the amount of NiO in the respective glasses. Glass MAST-N1 is the first to show the crystallization of α-cordierite while MAST-N5 is the last. Figure 9(b) shows the homogeneous needle-like microstructure for the α-cordierite in glass MAST-N1 heat treated at 1100 °C. Again the microstructure is in good agreement with the XRD as no other type of microstructure can be observed. A similar trend can be seen in the DTA thermographs of the glasses as there is a significant difference in the peak temperatures of crystallization for the final exotherms of glass MAST-N1 and MAST-N5. The second crystallization curve in the DTA thermographs of the glasses MAST-N1 and MAST-N3 is due to the formation of α-cordierite phase. The explanation for emergence of μ-C as the first crystalline phase and the hexagonal–orthorhombic transition in Mg-cordierite has already been explained in our previous study [19]. The lower T_{p2} and E_{c2} for glass MAST-N3 may be attributed to the increase in the liquid phase separation due to the increase in NiO, which led to the increase in the intensity of the crystallization in comparison to MAST-N1 after heat treatment at 950 °C (figure 7).

Also, the formation of MAS* at 950 °C and the decrease in the E_{c2} for MAST-N3 imply that the formation of α-cordierite via formation of a metastable phase MAS* is kinetically more favorable. The values of the Avrami parameter for the second crystalline phase $\langle n_2 \rangle$ for glasses MAST-N1 and MAST-N3 suggest that again the crystallization did not occur on a fixed number of nuclei and the crystalline phase, C, grows by the simultaneous surface and internal crystallization in glass MAST-N1, while three-dimensional bulk nucleation occurs in glass MAST-N3.

The formation of α-cordierite in MAST-N5 proceeded through the crystallization of a number of metastable phases at different temperatures. MAS remained the major crystalline phase until 1000 °C, but the intensity of the phase decreased considerably in the temperature interval 950–1000 °C. An unidentified phase (X) precipitated out at 950 °C and NS at 1000 °C as trace phases. A complete dissolution of the crystal structure occurred at 1050 °C, turning the glass–ceramic to an almost amorphous nature with very low intensity XRD peaks (150 cps) of Q and NS.

At 1100 °C, glass again was re-crystallized and sapphirine (S) precipitated out to be the single crystalline phase. The second crystallization curve of the DTA thermograph for glass MAST-N5 is probably due to the formation of this phase. The value of Avrami parameter for the second crystalline phase $\langle n_2 \rangle$ shows that the sapphirine grows by simultaneous surface and internal crystallization in the glass MAST-N5. At 1150 °C, the SiO_2 rich zone became highly stable and the crystalline nature of the glass–ceramic increased by three times (figure 8) with the emergence of cristobalite (Cb) as the major phase along with sapphirine (S) and α-cordierite (C) as the secondary phases.

No further change in the intensity and nature of the crystalline phases was observed even after heat treatment at 1200 °C (figure 9(c)). The higher activation energy of crystallization for the third crystallization peak of glass MAST-N5 also supports the XRD results as the value determined for E_{c3} is compounded corresponding to nucleation and growth processes or overlapping of two or more crystalline phases rather than specific to a single process. The value of Avrami parameter $\langle n_3 \rangle$ suggests that the crystalline phases corresponding to the final exotherm of glass MAST-N5 grow by one-dimensional surface nucleation and crystallization.

5. Conclusions

The results presented and discussed along this manuscript have shown that addition of NiO to near stoichiometric cordierite glasses nucleated with TiO_2 influences their thermal stability and crystallization kinetics, through the induced changes in phase separation kinetics and in the compositions of amorphous and crystalline phases. CTE and T_g for the glasses showed a decreasing trend with increasing NiO contents. All the three glasses behave as KS liquids but the value of F increases with NiO content increasing, pointing towards enhanced inhomogeneity in the glasses. The amount of NiO played a significant role in the crystallization behavior of the glasses through phase separation. At lower temperatures, irrespective of the added amount, NiO tends to remain in the glassy matrix. However, at higher temperatures it favors the segregation of SiO_2 rich zones that led to the formation of nickel silicate and quartz in glass MAST-N3 before the crystallization of α-cordierite phase. With the increase in NiO content to 5 mol%, SiO_2 rich zones became highly stable and did not get dissolved even at 1200 °C, thus leading to the formation of cristobalite as primary phase and near suppression of the α-cordierite phase. The activation energy of crystallization for μ-cordierite in all three glasses was found to be lower than the MAST glass and other stoichiometric cordierite glasses doped with B_2O_3 and P_2O_5. The calculated Avrami parameters for the different crystalline phases indicated that the growth of α-cordierite in MAST-N3 occurred through bulk nucleation

and crystallization while in the composition MAST-N5 it occurred through one-dimensional surface nucleation and crystallization. The growth of both μ- and α-cordierite in glass MAST-N1 took place through simultaneous surface and bulk nucleation and crystallization.

Acknowledgments

AG is grateful to CICECO and the University of Aveiro for the research grants.

References

[1] Grossman D G 1972 *J. Am. Ceram. Soc.* **55** 446
[2] Baik D S, No K S and Chun J S 1995 *J. Am. Ceram. Soc.* **78** 1217
[3] Baik D S, No K S, Chun J S, Yoon Y Y and Cho H Y 1995 *J. Mater. Sci.* **30** 1801
[4] Chaim R and Talanker V 1995 *J. Am. Ceram. Soc.* **78** 66
[5] Lee W E and Rainforth W M 1994 *Ceramic Microstructures: Property Control by Processing* (London: Chapman and Hall)
[6] Tummala R R 1991 *J. Am. Ceram. Soc.* **74** 895
[7] Knickerbocker S H, Kumar A H and Herron L W 1993 *Am. Ceram. Soc. Bull.* **72** 90
[8] Gregory A G and Veasey T J 1971 *J. Mater. Sci.* **6** 1312
[9] Sales M and Alarcon J 1995 *J. Mater. Sci.* **30** 2341
[10] Mccoy M A and Heuer A H 1988 *J. Am. Ceram. Soc.* **71** 673
[11] Awano M, Takas H and Kumahara Y 1992 *J. Am. Ceram. Soc.* **35** 2535
[12] McMillan P W 1979 *Glass–Ceramics* 2nd edn (London: Academic)
[13] Lachman I M 1986 *Sprechsaal* **119** 1116
[14] Golubkov V V, Chuvaeva T I, Dymshits O S, Shashkin A A, Zhilin A A, Byun W–B and Lee K–H 2004 *J. Non-Cryst. Solids* **345/346** 187
[15] Golubkov V V, Dymshits O S, Zhilin A A, Chuvaeva T I and Shashkin A V 2004 *Glass Phys. Chem.* **30** 300
[16] Alekseeva I, Dymshits O, Golubkov V, Shashkin A, Tsenter M, Zhilin A and Byun W B 2005 *Glass Technol.* **46** 187
[17] Boberski C and Giess E A 1994 *J. Mater. Sci.* **29** 67
[18] Doenitz F D, Russ C and Vogel W 1982 *J. Non-Cryst. Solids* **53** 315
[19] Goel A, Shaaban E R, Melo F C L, Ribeiro M J and Ferreira J M F 2007 *J. Non-Cryst. Solids* **353** 2383
[20] Macmillan J A 1965 *J. Phys. Chem.* **42** 3497
[21] Mahadevan S, Giridhar A and Singh A K 1986 *J. Non-Cryst. Solids* **88** 11
[22] Weyl W A 1951 *Coloured Glasses* (Sheffield: Soc. Glass Technol.) p 558
[23] Calas G, Cormier L, Galoisy L and Jollivet P 2002 *C. R. Chimie* **5** 831
[24] Chou Y-S, Stevenson J W and Gow R N 2007 *J. Power Sources* **168** 426
[25] Lide D 2004 *CRC Handbook of Chemistry and Physics* 84th edn (Boca Raton, FL: CRC Press)
[26] Wu J-M and Hwang S-P 2000 *J. Am. Ceram. Soc.* **83** 1259
[27] Vázquez J, Wagner C, Villares P and Jiménez-Garay R 1998 *J. Non-Cryst. Solids* **235–237** 548
[28] Francis A A 2005 *J. Am. Ceram. Soc.* **88** 1859